Random dynamical system in time domain: A POD-PC model

Version of Record: https://www.sciencedirect.com/science/article/pii/S0888327019304662
Manuscript_6669c1ff05e49e39e0874289307b9d15

Random dynamical system in time domain: a POD-PC model

E. Jacquelin[a,*], N. Baldanzini[b], B. Bhattacharyya[a], D. Brizard[a], M. Pierini[b]

[a] *Univ Lyon, Université Claude Bernard Lyon 1, IFSTTAR, LBMC UMR-T9406, F69622, Lyon, France*
[b] *Department of Industrial Engineering, University of Florence, Firenze, Italy*

Abstract

Propagating uncertainties through mechanical systems has been widely studied for the last thirty years. In particular metamodels based on polynomial chaos expansion (PCE) have been successfully developed in the context of both intrusive and non-intrusive methods. However, modelling random dynamical systems is much more challenging and requires increasing computational resources when the time integration becomes longer. Therefore separating the time aspect of the dynamical response and the random contributions is an appealing approach, which has been used in this paper. Thus, a non-intrusive method is proposed by associating a proper orthogonal decomposition (POD) and a PCE. The POD-PC model was applied on three examples. On two examples, the method was very efficient not only in calculating the first two statistical moments, but also in estimating the responses corresponding to several samples of the random parameters. As to the last example, the Kraichnan-Orszag three-mode problem, the model was able to estimate well the evolution of the first two statistical moments for the first part of the time duration, but a noticeable discrepancy occurred for the remaining part. It seems that the model is more appropriate to estimate the transient response of a random dynamical system than the steady-state response.

Keywords: Random dynamical systems; structural dynamics; uncertainty propagation; proper orthogonal decomposition; polynomial chaos expansion.

1. Introduction

Describing random dynamical systems is still a challenge that arises in many engineering problems, despite the progresses made in the late thirty years. The main recent

*Corresponding author: eric.jacquelin@univ-lyon1.fr, Tel: +33478931671

developments for modelling uncertain systems essentially concern the Polynomial Chaos (PC) Expansion (PCE) method. The latter has gained a strong popularity since the works by Ghanem and Spanos [1].

Despite many successful applications of the PCE for evaluating the response of linear random dynamical systems in transient regime [2] or in frequency domain [3], it was shown by several authors that the method [4–6] is not adapted when long-time integration is required. Making use of the periodicity of the solutions, some transformations (either in the phase space or in the time domain), together with a PCE, were used to obtain in-phase solutions, and then to evaluate random limit cycle oscillations and long-time integration response [5, 7, 8]. This method was developed further in a non-intrusive context [9]. While these methods are dedicated to specific problems, a more general procedure is presented in [6]: considering the drawbacks are a consequence of the statistical response evolution with time, it is proposed to update the PC basis when it becomes not optimal to describe the response distribution. This method is attractive, but may not be effective when the basis must be often updated. Other approaches based on wavelet or Wiener-Haar expansion were also used [4, 10].

A black-box method has been proposed in [11, 12] based on a nonlinear autoregressive exogenous (NARX) model: this approach may be efficient as it separates the random and time variables, but identifying the NARX structure is not easy. It turns out that separating variables in function of their nature (space, time, randomness) belongs to a class of efficient methods, the Proper Generalized Decomposition (PGD) methods [13]. They have been recently developed in the context of uncertainty propagation with the generalized spectral decomposition in [14]. The latter has been extended for random time dependent problem in [15] and similarities with the proper orthogonal decomposition (POD) were observed: unlike the latter, the former builds an a priori basis for representing the solution.

These methods are not directly applicable for non-intrusive methods or for data coming directly from experiments, where the mathematical model is not known. However a posteriori information is known in both cases either with the many simulations of a deterministic code (non-intrusive methods) or with measured data (experiments). Therefore,

the POD can be applied to obtain a basis of representation that decouples the variables. Thus, in [16–18] a principal component analysis or a POD was used to separate randomness from the others variables in a non-intrusive way. In [17], it was clear to the authors that the method can be used for random dynamic problem, but they did not investigated the method. Therefore, this study aims to address the applicability of the POD-PC method to an uncertain dynamical systems.

The paper is organized as follows. After giving in section 2 the main notations, in section 3 the PCE and the POD are briefly introduced, and the combination of both methods is presented. In section 4 several examples are presented. Finally in section 5 some conclusions are drawn.

2. Notations

m number of random parameters

ξ random m-vector; element ξ_i is a random variable that has a one-to-one correspondence with one uncertain parameter

$\mathcal{M}(\xi)$ mathematical or numerical model, which depends on random vector ξ

$x = \mathcal{M}(\xi)$ response of model $\mathcal{M}$: both the model and the response can be time dependent

Ξ any sample of ξ

$\mathbf{\Xi}$ $N \times m$ design of experiment (DoE) matrix; row i, $\mathbf{\Xi}_i$, is a sample of ξ; column j collects N samples of ξ_j

t time; t is discretized in n_t values, $\{t_i\}_{i=1,\cdots,n_t}$

$x(t, \Xi)$ response at time t when the random parameters are set to Ξ

$\mathbf{x}(\Xi)$ n_t-vector, which corresponds to the time discretized $x(t, \Xi)$

$\mathbf{x}(\mathbf{\Xi})$ $n_t \times N$-matrix: column i is the time discretized response when the random parameters are set to sample $\mathbf{\Xi}_i$

$$\forall i = 1, \cdots, n_t \ \forall j = 1, \cdots, N \quad \mathbf{x}(\mathbf{\Xi})_{i,j} \ = \ x(t_i, \mathbf{\Xi}_j) \tag{1}$$

3. PCE and POD models

3.1. Polynomial chaos expansion

A polynomial chaos expansion consists in finding the response of a model as an expansion on a polynomial orthogonal basis that depends on ξ [1]

$$x(\xi) \;=\; \sum_{J\in\mathbb{N}^m} Y_J \; \Psi_J(\xi) \tag{2}$$

where:

- J is a multi-index $J = (J_1, \cdots, J_m)$; $|J| = \sum_{i=1}^{m} J_i$ is the order of polynomial Ψ_J.
- $\Psi_J(\xi) = \prod_{j=1}^{m} \psi_{J_j}(\xi_j)$
- $\psi_{J_j}(\xi_j)$ belongs to an orthogonal polynomial family; the orthogonality is with respect to the probability measure related to random variable ξ_j; the choice of the family is related to the probability distribution of ξ_j (e.g., Legendre polynomial if ξ_j has a uniform distribution).

In practice the series is truncated up to order P and the approximate solution x^P is an expansion over $\mathbb{I}^P$, a set of multi-index J such that $\mathbb{I}^P = \{J \in \mathbb{N}^m / |J| \leq P\}$. The cardinality of $\mathbb{I}^P$ is denoted n_P, which depends on P and m: $n_P = (m+P)!/(m!\,P!)$. x^P can be cast as [19]

$$x(\Xi) \;\simeq\; x^P(\Xi) \;=\; \sum_{J\in\mathbb{I}^P} Y_J \; \Psi_J(\Xi) \;=\; \sum_{j=1}^{n_P} Y_j \; \Psi_j(\Xi) \tag{3}$$

where j referred to the j-th element of $\mathbb{I}^P$. To make the notations clearer x^P is denoted by x in the following, but obviously all the PCE results are related to a truncated PCE.

The main difficulties are to find the proper order P and also to select, within the terms of the expansion, which ones are the most relevant. Indeed, it turns out that a large number of terms in the expansion is unnecessary. In addition, considering too many terms with a high polynomial degree may give overfitting. Finally, the selection of the more relevant terms leads to a sparse representation involving n_P^{sparse} terms instead of n_P terms

($n_P^{sparse} \leq n_P$), which increases the computation speed. Many methods exist to achieve a sparse representation of a polynomial chaos basis. A least angle regression algorithm [20] together with a cross-validation criterion is used in [21–23]. An alternative method is based on a Bayesian approach and the so-called automatic relevance determination [23–25]: it has been used in this study.

The coefficients of the PCE can be determined by several methods, which may be categorized in intrusive methods and non-intrusive methods. The former [26–28] consists mainly in substituting expansion (2) in the equations, which are then projected on the PC: the coefficients are the solution of the obtained system. The non-intrusive methods lay on N evaluations of the model for the N samples of the DoE, $\mathbf{\Xi}$; amongst several non-intrusive methods, a popular one is a regression method [29–31]

$$\hat{\mathbf{x}}(\mathbf{\Xi}) \;=\; \mathbf{\Psi}(\mathbf{\Xi})\ \mathbf{Y} \tag{4}$$

where $\hat{\mathbf{x}}(\mathbf{\Xi})$ is a N-vector of the N model evaluations; $\mathbf{Y}$ is the n_P-vector of the n_P PCE coefficients; $\mathbf{\Psi}(\mathbf{\Xi})$ is a $N \times n_P$ matrix: element (i, j) is the evaluation of the j-th PC for the i-th sample of $\mathbf{\Xi}$. Solving Eq.(4) gives $\mathbf{Y}$.

3.2. PCE in time domain

A PC model in time domain can be built as it was done with Eq. (3)

$$x(t, \xi) \;=\; \sum_{j=1}^{n_P} Y_j(t)\ \Psi_j(\xi) \tag{5}$$

Each coefficient of the PCE depends on the time. In practice it means that each coefficient $Y_j(t)$ must be determined at each time step [28]: therefore, n_t PCE models should be determined. This procedure can have a quite large numerical cost when the number of time steps is large.

As already mentioned, some authors [5, 6] pointed out that a PCE may fail for long-time integration when an intrusive method is used.

In Eq. 5, polynomials Ψ_j are known and the time dependent coefficient must be

estimated. An alternative would consist in finding an expansion:

$$x(t,\xi) \;=\; \sum_{i=1}^{n_V} a_i(\xi)\; V_i(t) \tag{6}$$

where time dependent functions $V_i(t)$ are known and coefficients $a_i(\xi)$ are the unknowns. The proper orthogonal decomposition offers a way to estimate $V_i(t)$ in a non-intrusive way.

3.3. Proper orthogonal decomposition

Proper orthogonal decomposition has been widely used in turbulence [32] to detect the "coherent structures" in a turbulent flow. The objective is similar in this study. Indeed when a random DoE, $\mathbf{\Xi}_{tr}$, is chosen to train the model, as long as no bifurcation occurs [7], the related responses, $\mathbf{x}_{tr} = \mathbf{x}(\mathbf{\Xi}_{tr})$ ($n_t \times N$-matrix), often look similar. Therefore, it is possible to extract the "coherent" time shapes from $n_t \times n_t$-matrix $\mathbf{S}$

$$\mathbf{S} \;=\; \mathbf{x}_{tr}\; \mathbf{x}_{tr}^T \tag{7}$$

where "T" stands for the transpose matrix.

Matrix $\mathbf{S}$ is often considered as a kind of correlation matrix. It turns out that the set of the eigenvectors $\{\mathbf{V}_i\}_{i=1,\dots,n_t}$ of $\mathbf{S}$, which are gathered in matrix $\mathbf{V}$, is an interesting orthogonal basis [32, 33]. The vectors verify

$$\forall i = 1, \cdots, n_t \quad \mathbf{S}\; \mathbf{V}_i \;=\; \lambda_i^2 \mathbf{V}_i \tag{8}$$

POD-values $\lambda^2 = \{\lambda_i^2\}_{i=1,\dots,n_t}$ are useful as each one represents a so-called [34] energy involved along the POD-vector $\mathbf{V}_i$ direction: their relative values indicate the relative importance between two POD-components. In the following each vector $\mathbf{V}_i$ has a unit norm and they are sorted according to the decreasing values of λ_i^2: accordingly V_1 is often similar to the response mean.

Each POD-vector $\mathbf{V}_i$ has n_t element. Therefore, the random response can be represented by Eq. (6), with $n_V = n_t$:

$$\mathbf{x}(t,\xi) \;=\; \sum_{i=1}^{n_t} a_i(\xi)\; \mathbf{V}_i(t) \tag{9}$$

It can also be noticed that $\mathbf{V}$ and λ can also be obtained with a singular value decomposition (SVD) of $\mathbf{x}_{tr}$. Therefore, as N is usually lower than n_t, $\forall i > N$, λ_i is equal to zero. Consequently, only the first N POD modes are interesting to describe the response, as the other ones do not bring any energy. Furthermore, in practice the responses can be described accurately with the first n_a ($n_a < N$ and often $n_a << N$) eigenvectors as most of the energy is concentrated in these vectors

$$\mathbf{x}(t,\xi) \simeq \sum_{i=1}^{n_a} a_i(\xi)\ \mathbf{V}_i(t) \tag{10}$$

n_a is often chosen so that 99 % of the POD-energy remains in the approximation [32, 35], i.e. $\sum_{i=1}^{n_a} \lambda_i^2 \geq 0.99 \sum_{i=1}^{N} \lambda_i^2$; in [36], it is proposed to keep "99.9 %" of the energy. The "99 %" criterion will be addressed in the examples.

3.4. POD-PC model

The coefficients of expansion (10) are random and are estimated with a PCE

$$a_i(\xi) = \sum_{j=1}^{n_P} A_{ij}\ \Psi_j(\xi) \tag{11}$$

It can be noticed that a Gaussian process approach was used in [16] to estimate the coefficients.

Due to the orthonormality of the basis, projecting Eq. (10) on POD-vector $\mathbf{V}_i$ gives

$$a_i(\xi) = \mathbf{x}(\xi)^T\ \mathbf{V}_i \tag{12}$$

Using response vector $\mathbf{x}(\mathbf{\Xi}_{tr})$, Eq. (12) provides a collection of N samples for each a_i, which are gathered in vector $\mathbf{a}_i$. Therefore, coefficients A_{ij} are evaluated by solving

$$\mathbf{a}_i = \mathbf{\Psi}(\mathbf{\Xi}_{tr})\ \mathbf{A}_i \tag{13}$$

where $\mathbf{A}_i$ is the PCE coefficient vector of a_i.

The response of a random dynamical system is then eventually described by the following POD-PC model

$$\mathbf{x}(t,\xi) \simeq \sum_{i=1}^{n_a} \sum_{j=1}^{n_P} A_{ij}\ \Psi_j(\xi)\ \mathbf{V}_i(t) \tag{14}$$

All the steps of the POD-PC procedure are gathered in Algorithm 1.

Using a sparse PCE instead of a full PCE gives

$$\mathbf{x}(t,\xi) \simeq \sum_{i=1}^{n_a} \sum_{j=1}^{n_P^{sparse}} A_{ij}\ \Psi_j(\xi)\ \mathbf{V}_i(t) \tag{15}$$

In that case, the least square regression in STEP 5 of Algorithm 1 is replaced by the sparse method to identify the non-null coefficients and their evaluation.

Algorithm 1 POD-PC model

INPUT: N; n_P; $\mathbf{\Xi}_{tr} \in \mathbb{R}^{N\times m}$
OUTPUT: A_{ij}: Eq. (14)

STEP 1: model evaluation; PC evaluation
for $i \leftarrow 1$ to N **do**
  $\mathbf{x}_{tr}(:,i) = \mathcal{M}(t, \mathbf{\Xi}_{tr}(i,:)$
  $\mathbf{\Psi}_{tr}(i,:) = \mathbf{\Psi}(\mathbf{\Xi}_{tr}(i,:))$
end for
$\mathbf{x}_{tr} \in \mathbb{R}^{n_t\times N}$
$\mathbf{\Psi}_{tr} \in \mathbb{R}^{N\times n_P}$

STEP 2: POD eigenvectors and eigenvalues
Evaluate $(\mathbf{V}, \lambda) = \text{svd}(\mathbf{x}_{tr})$

STEP 3: truncature of the POD
Find n_a such that $\sum_{i=1}^{n_a} \lambda_i^2 \geq \alpha \sum_{i=1}^{N} \lambda_i^2$; usually $\alpha = 0.99$
$\forall i \in 1, \cdots, n_a \quad \mathbf{V}_i = \mathbf{V}(:,i)$

STEP 4: samples of POD coefficients
for $i \leftarrow 1$ to n_a **do**
  $\mathbf{a}_i = \mathbf{x}_{tr}^T \mathbf{V}_i$
end for

STEP 5: PCE coefficients
for $i \leftarrow 1$ to n_a **do**
  $\mathbf{A}_i = \mathbf{\Psi}_{tr} \setminus \mathbf{a}_i$ {least square regression}
end for

4. Examples

Three different examples are proposed. The first one is related to a real case and the uncertainties are given in the standard. The responses of the second example are given

by a random ordinary differential equation and deform considerably when the random parameter varies; nevertheless, at each instant the variation of the response in function of the random variable is monotonic and smooth. The third example involves a long time integration.

4.1. Helmet impact test

This study addresses the homologation tests for motorcycle helmets described in the ECE 22.05 regulation [37]. Such tests consist in impacts of the helmet, fitted with an instrumented headform, at a specified velocity and positions on a rigidly fixed anvil. As such a test can not occur perfectly, uncertainties related to the position and the impact velocity are given in the standard. The uncertain position is described with two angles, which give the possible rotations (front/rear, left/right) of the helmet with respect to the nominal position. The impact parameters and uncertainties are listed in Table 1.

One impact point was selected for this study: the "forehead" of the helmet. The calculations were carried out with a finite element model of the helmet developed at Università degli Studi di Firenze [38] on the LS-DYNA explicit solver. The impact test is calculated for 29.9 ms and the outputs are written every 0.1 ms. The quantity of interest is the acceleration of the headform along the direction of the initial velocity.

To pass the impact test [37], the peak acceleration of the headform must remain below 275 g (where g is the standard gravity), and the head injury criterion (HIC) must be lower than 2400, where this quantity is defined as

$$HIC \;=\; \max_{t_1,t_2} \left\{ \left[\frac{1}{t_2 - t_1} \int_{t_1}^{t_2} x(t)dt \right]^{2.5} (t_2 - t_1) \right\} \tag{16}$$

with $t_2 - t_1 \leq 36$ ms, and acceleration x (resp. time t_1, t_2) is given in g (resp. in seconds).

impact velocity	v_i	[7.5, 7.65]	m/s
x-angle	α_x	[-3, 3]	°
y-angle	α_y	[-3, 3]	°

Table 1: Ranges of the three uncertain parameters

A DoE matrix was build with 60 samples of the three uncertain parameters drawn according to uniform laws, with the bounds given in Table 1, with a Latin Hypercube Sampling (LHS) method and 60 samples of the acceleration were therefore calculated. The

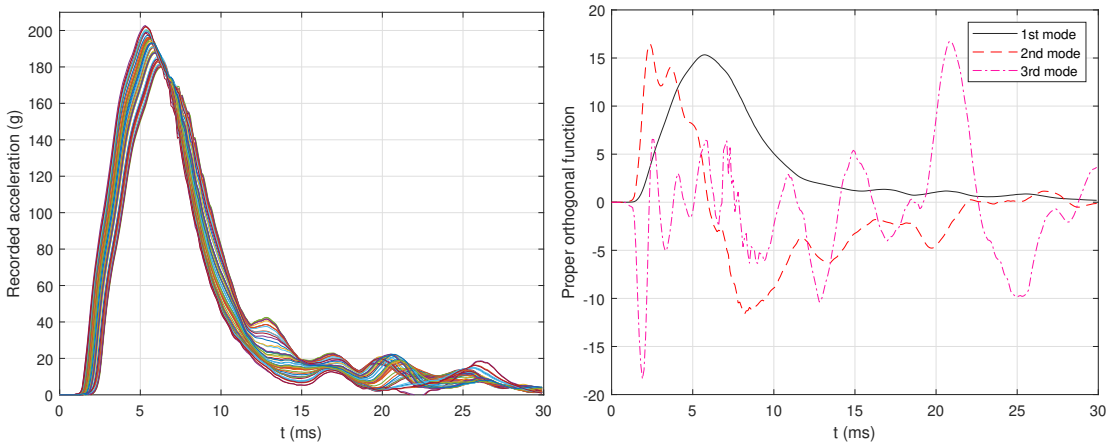

(a) (b)

Figure 1: (a): 50 samples of acceleration; (b) first three proper orthogonal functions: $V_1(t)$ in black solid line, $V_2(t)$ in red dashed line, $V_3(t)$ in magenta dash-dotted line

POD-PC procedure was applied with 50 samples of the acceleration drawn randomly from the 60 samples: the 10 remaining samples were used to validate the model. Figure 1(a) shows a progressive deformation of the acceleration curve when the random parameters vary. The first three proper orthogonal function, $V_i(t)$, are plotted in Fig. 1(b). It can be seen that the first one is very close to the global shape of the accelerations.

Legendre polynomials were used as all the random variables have a uniform distribution. Each PCE coefficient vector $\mathbf{A}_i$ defined in Eq. (14) was identified from 50 samples of a_i calculated with Eq. (12) and a PCE order lower or equal to 4 ($n_P = 35$). The quality of the POD-PC procedure is tested on the 10 remaining samples of the acceleration time series: the actual responses (i.e., obtained with the LS-DYNA model) were compared to the identified ones obtained with the POD-PC model and plotted in Fig 2. A relative error, err, was calculated between both responses over the 10 samples

$$err = \frac{\|x_{\text{actual}} - x_{\text{identified}}\|_2}{\|x_{\text{actual}}\|_2} \tag{17}$$

The maximum number of terms in the sparse PCE involved in evaluating all the coefficients a_i (Eq. (11)), $n_P^{sparse}|_{max}$, the ratio of the remaining energy to the total energy in the POD, r_{energy}, and n_a are listed in Table 2. It can be seen than 99.99 % of the POD energy remains in the approximation with only $n_a = 8$ terms over the 50 possible terms.

To check the robustness of the model, the procedure was repeated many times: it means that several groups of 50 samples were used to identify the model. The error has

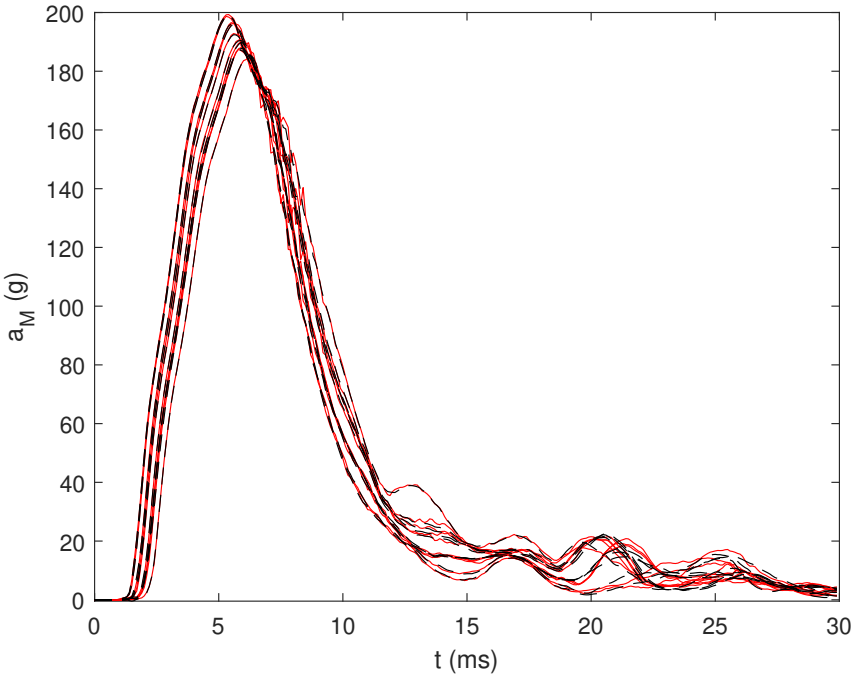

Figure 2: Identified (black dashed line) and actual (red solid line) acceleration in time domain

$n_P^{sparse}\|_{max}$	r_{energy} (%)	n_a	err (%)
9	99.99	8	1.2

Table 2: sparse POD-PC approximation parameters

changed very little and remained between 0.8 to 1.2 %.

In order to test the efficiency of the POD-PC model, The HIC was also calculated from both the actual and identified accelerations from Eq. (16). The results are presented in Fig. 3 where the identified values are given as a function of the actual ones: the closest the points to the first bisector of the plot, the more accurate the model. It can be seen that the values of HIC obtained from the POD-PCE model were very close to the actual values: the relative error was about 0.25 %.

The initial budget for this example was for 60 model evaluations (50+10 for validation). A study on the evolution of the HIC error with samples ranging from 2 up to 50 was performed. Fig. 4 shows that even with $N = 15$ the error is already lower than 0.6 %.

4.2. First order ordinary differential equation (ODE)

Consider the following first order random ode

$$\frac{\mathrm{d}x(t)}{\mathrm{d}t} + k\ x(t) = 0, \qquad x(t=0) = 1 \tag{18}$$

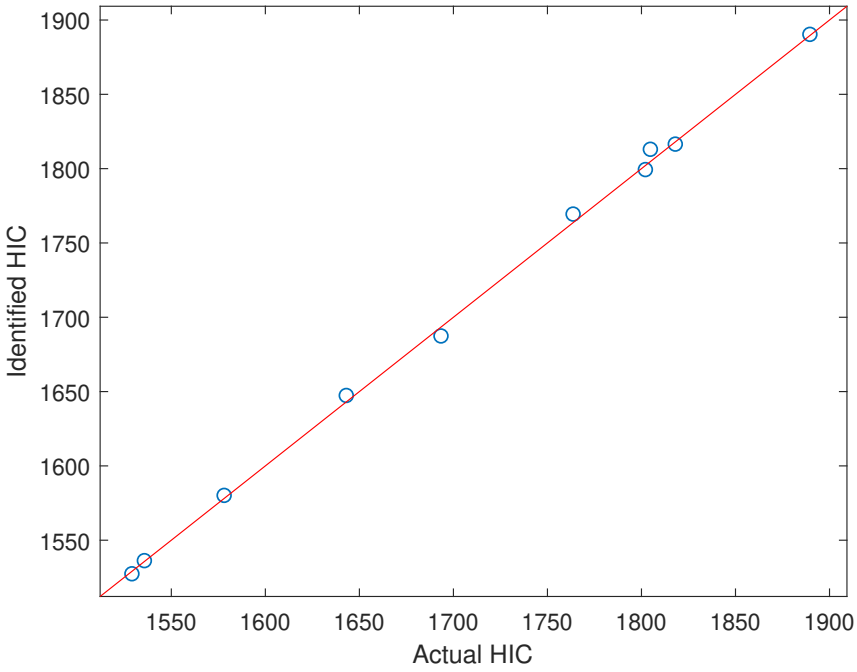

Figure 3: Blue circles: scatterplot of identified and actual HIC; red solid line: first bisector

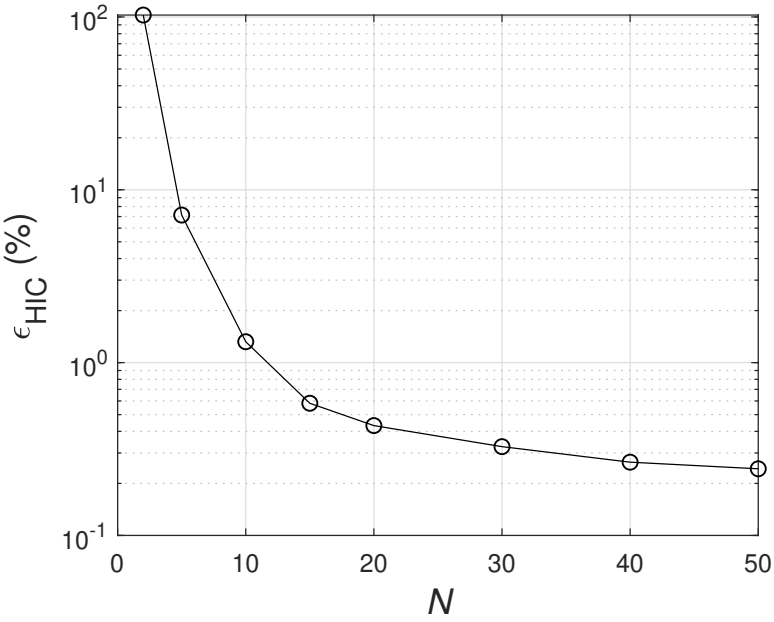

Figure 4: HIC error

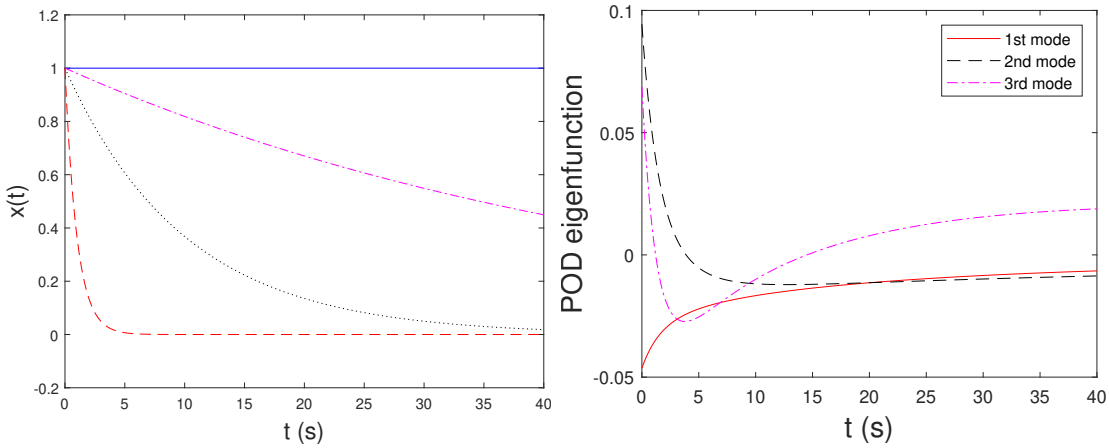

(a) (b)

Figure 5: (a): 1st order ode solution for several samples of k: $k = 0$ (blue solid line), $k = 0.02$ (magenta dash-dotted line), $k = 0.1$ (black dotted line), $k = 1$ (red dashed line); (b) first three proper orthogonal functions: $V_1(t)$: black solid line, $V_2(t)$: red dashed line, $V_3(t)$: magenta dash-dotted line

where k is a random variable with a uniform distribution in [0 1]. This equation has been studied several times [6, 26, 39], and is interesting because the solution as well as the mean ($\overline{x}$) and the variance (σ_x^2) have an analytical expression

$$x(t) = \exp(-k\,t) \tag{19}$$

$$\overline{x}(t) = \frac{1-\exp(-t)}{t} \tag{20}$$

$$\sigma_x^2(t) = \frac{1-\exp(-2t)}{2t} - \left(\frac{1-\exp(-t)}{t}\right)^2 \tag{21}$$

Contrary to the previous example, the shape of the curves changes a lot between $k = 0$ and $k = 1$ (see Fig. 5(a)). The first three proper orthogonal functions are plotted in Fig. 5(b).

Algorithm 1 was applied:

- **INPUT:** $N = 40$ samples of random variable k are drawn according to a uniform law over [0, 1] with a LHS method; $m = 1$ and $d = 15$, then $n_p = 16$; $\mathbf{\Xi}_{tr} = 2k-1 \in \mathbb{R}^{40\times 1}$
- **STEP 1a:** For each sample of $\mathbf{\Xi}_{tr}$, Eq. (18) is solved ($n_t = 4001$ and $t \in [0,\ 40]$ s): the solution are collected in matrix $\mathbf{x}_{tr} \in \mathbb{R}^{4001\times 40}$
- **STEP 1b:** Legendre polynomials are used; $\mathbf{\Psi}(\mathbf{\Xi}_{tr}) \in \mathbb{R}^{40\times 16}$ is evaluated for each sample of $\mathbf{\Xi}_{tr}$

- **STEP 2:** The SVD of $\mathbf{x}_{tr}$ provides $(\mathbf{V}, \lambda)$; $\mathbf{V} \in \mathbb{R}^{4001\times 40}$; $\lambda \in \mathbb{R}^{40\times 1}$
- **STEP 3:** $n_a = 3$ POD modes were kept with the 99 % criterion; $\mathbf{V}_i \in \mathbb{R}^{4001\times 1}$
- **STEP 4:** $\forall i = 1, \cdots, n_a = 3$ compute $\mathbf{a}_i = \mathbf{x}_{tr}^T \mathbf{V}_i$; $\mathbf{a}_i \in \mathbb{R}^{40\times 1}$
- **STEP 5:** PCE coefficients of $\mathbf{a}_i$, $\mathbf{A}_i$, are evaluated with a sparse procedure.

As proposed at STEP 1 of the procedure, a PCE of degree 15 was necessary to identify the POD expansion coefficients. It was found that the PCE was not sparse as each coefficient $a_i(\xi)$ had an expansion with at least n_P^{sparse} =14 terms over the n_P =16 terms present in the full PCE.

The above-mentioned criterion specified to determine the efficient number of POD indicates that three POD modes should estimate the theoretical solutions. To verify the quality of the POD-PC model, the mean and the variance of the response were plotted (see Figs. 6(a)-6(c)) as well as one sample of the solution (Fig. 6(e)) for both the analytical and the POD-PC solutions. It clearly appears that, except for the mean, the estimations are not excellent, despite $\sum_{i=1}^{3} \lambda_i^2/\lambda_{max}^2 > 99.6\%$: it seems that the criterion should be changed. Therefore all the POD modes such that $\lambda_i/\lambda_{max} > 10^{-5}$ were finally kept: for all the cases tested, this criterion is such that $\sum_{i=1}^{n_a} \lambda_i^2/\lambda_{max}^2 > 99.99\%$. In the present example, 6 POD modes are kept in the analysis. The results are in excellent agreement with the theoretical results, as it may be seen in Fig. 6. In particular, the relative error between the actual response and the identified one for the sample represented in Figs. 6(e)-6(f) was equal to 10.6 % with 3 modes and to 0.4 % with 6 POD modes. In Figure 7, it can be seen that, with 6 POD modes, the error is almost the lowest error possible; above 7 POD modes, almost 100 % of the energy is kept.

The $\lambda_i/\lambda_{max} > 10^{-5}$ criterion is applied in the rest of the paper.

4.3. Kraichnan-Orszag three-mode problem

The Kraichnan-Orszag system has been used many times [6, 39, 40] since the first study with the Wiener-Hermite expansion [41]. It consists in nonlinear differential equations with uncertain initial conditions:

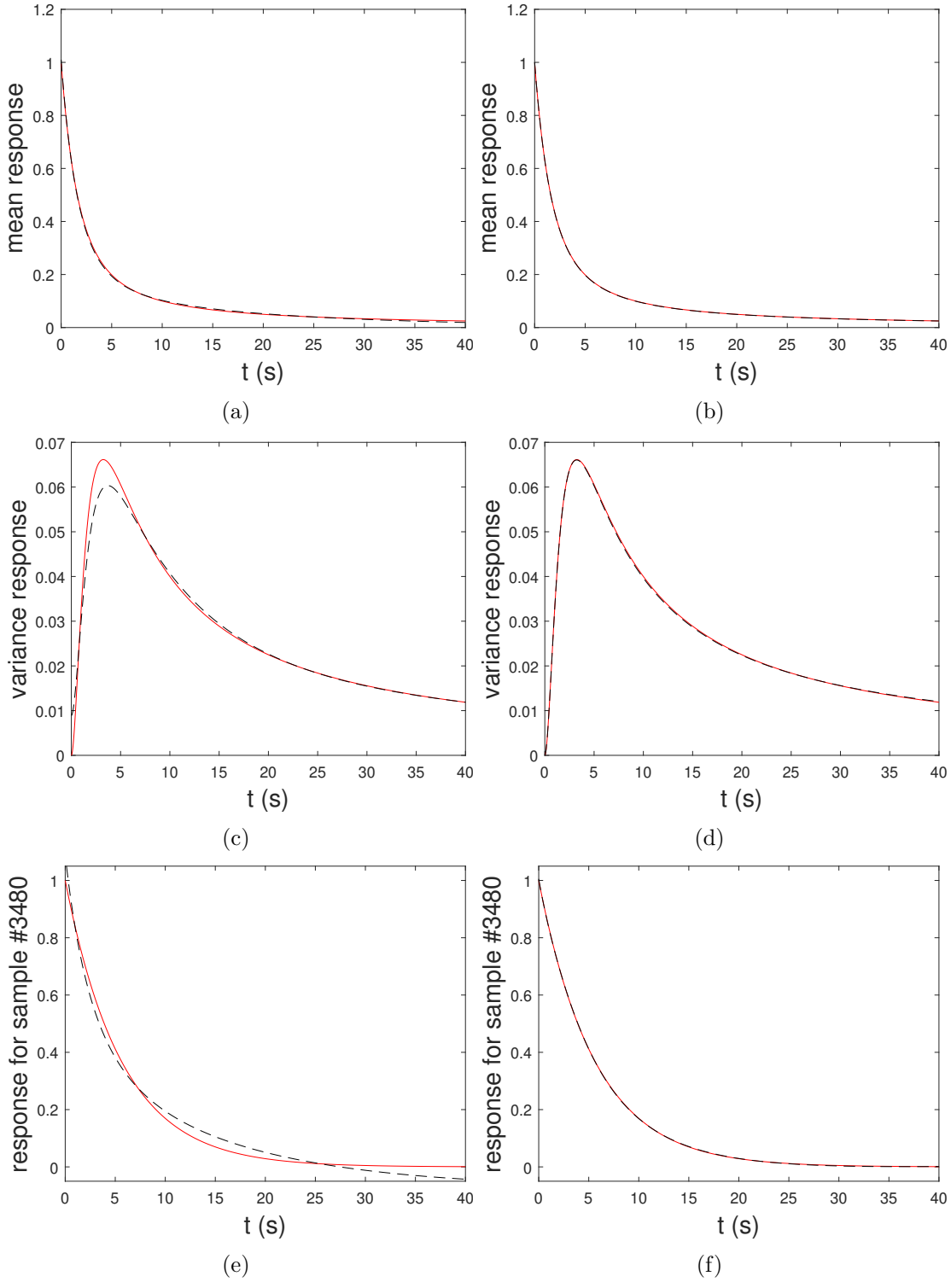

Figure 6: 1st order ode solution with analytical solution (red solid line) and the POD-OC model (black dashed line); mean solution (a): $n_a = 3$, (b): $n_a = 6$; variance of the solution (c): $n_a = 3$, (d): $n_a = 6$; 3480-th sample of the solution (e): $n_a = 3$, (f): $n_a = 6$

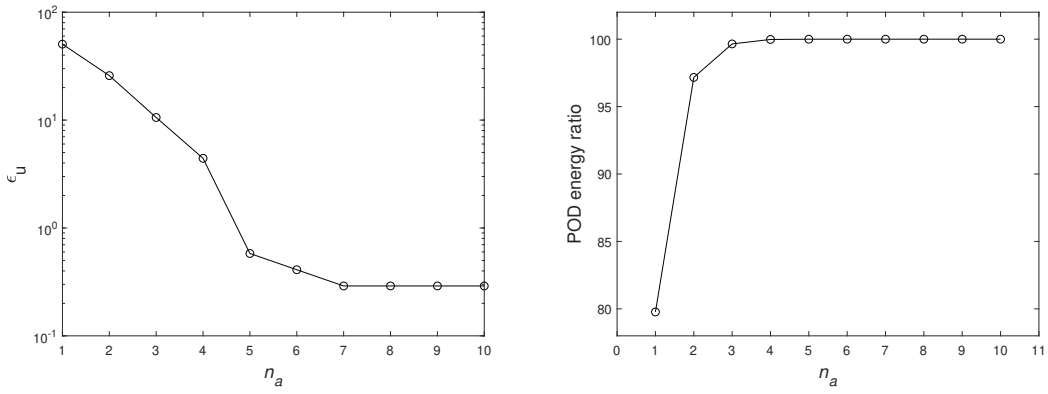

(a) (b)

Figure 7: Evolution of (a) the error on u, (b) POD energy ratio

$$\frac{\mathrm{d}x_1}{\mathrm{d}t} = x_2\ x_3 \tag{22}$$

$$\frac{\mathrm{d}x_2}{\mathrm{d}t} = x_3\ x_1 \tag{23}$$

$$\frac{\mathrm{d}x_3}{\mathrm{d}t} = -2\ x_1\ x_2 \tag{24}$$

with $\forall i \in \{1,2,3\},\quad x_i(0) = \alpha_i + \beta_i\ \xi_i$, where ξ_i is a uniformly random variable on the interval [-1,1] and α_i, β_i are constants, which have the following values in this study

$$\alpha_1 = 0.99 \text{ or } 0.995$$

$$\alpha_2 = \alpha_3 = 1$$

$$\beta_1 = 0.01$$

$$\beta_2 = \beta_3 = 0$$

As β_2 and β_3 are zero, the studied problem is a 1 random variable problem. The solution is very sensitive to the value of $x_1(0)$ and then to α_1: therefore when $\alpha_1 = 0.995$ two families of solution can be seen as $x_1(0)$ can be greater or lower than 1, which is a limit point, whereas only one family is possible when $\alpha = 0.99$. This is shown in Fig. 8 where the response of the system was obtained for 5 different samples of ξ_i for both values of α_1 (red solid lines). It was then expected that the results would be more difficult to reproduce with $\alpha_1 = 0.995$.

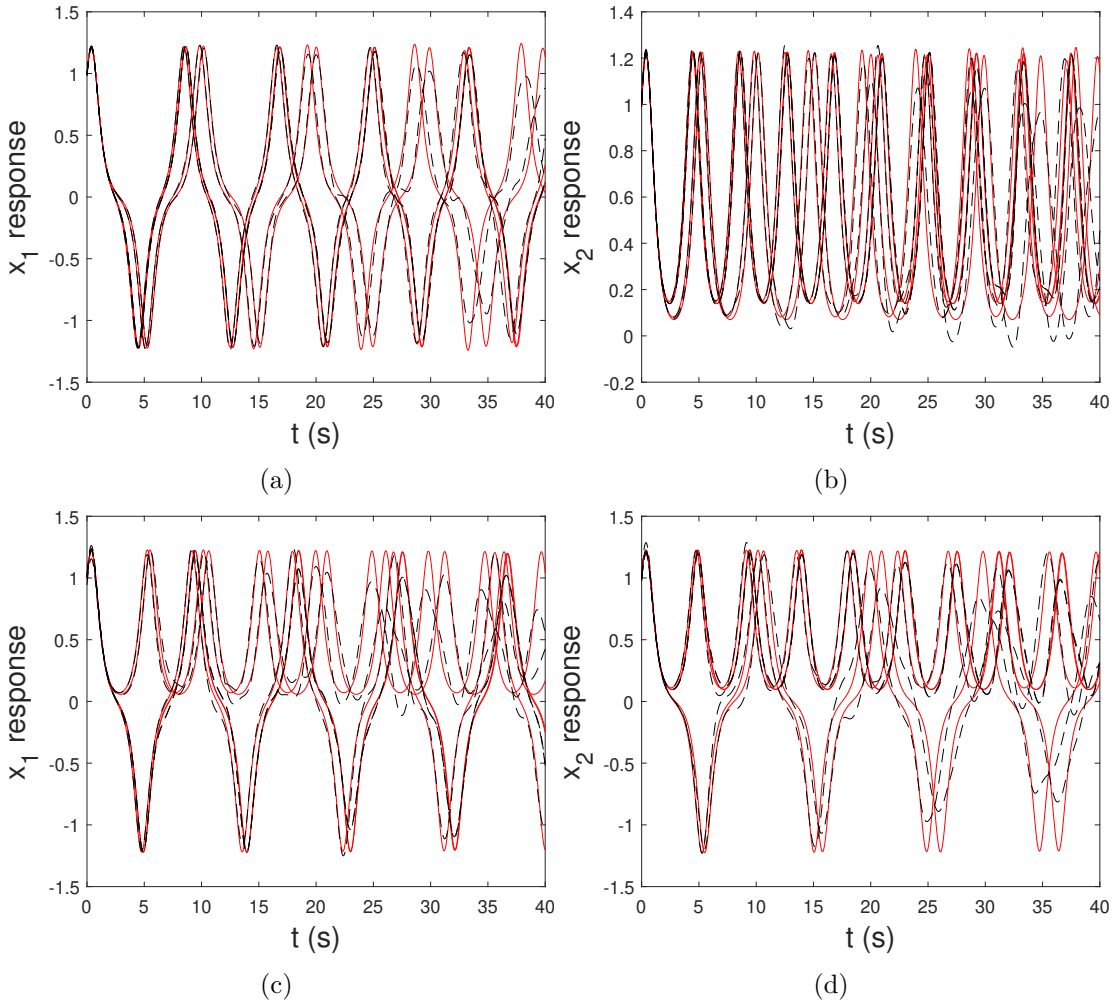

Figure 8: Comparison direct simulations (red solid line) vs. POD-PC method (black dashed line) for 5 samples: α=0.990, response of x_1 (a), response of x_2 (b); α=0.995, response of x_1 (c), response of x_2 (d)

α_1	0.990	0.995
$\bar{x}_1$	1.83	4.86
$\bar{x}_2$	1.46	2.90
$\bar{x}_3$	1.36	3.30
σ_{x_1}	4.23	9.57
σ_{x_2}	5.89	13.39
σ_{x_3}	2.74	11.67

Table 3: Relative error (in %) on the mean response ($\bar{x}_i$) and the variance response (σ_{x_i}) computed with POD-PC for both values of α_1.

The POD-PC model was derived for both values of α_1. Eqs (22-24) were solved with a time step dt =0.01 s for 40 s; smaller time steps were also used without changing the results. The POD-PC model calculated with N=200 initial samples; Legendre polynomials were used and a PC order P=20 gave the response mean and variance plotted in Figs. 9-10 as well as the results obtained with a Monte Carlo simulation (MCS), with 10000 samples of α_1 drawn with a LHS method. Fig. 8 shows the response obtained with both the POD-PC method and the direct simulation, for 5 several samples.

The errors listed in Table 3 and Figs. 9-10 show that the mean is always very well estimated with the POD-PC model, even for α_1=0.995. However, if the variance is well estimated for α_1=0.99, Fig. 10 shows a discrepancy that increases with time for α_1=0.995 and the relative error reaches 13.4 % for x_2 (see Table 3). Therefore the accuracy is not as good as the one presented in [6], which has even been improved in [40]; on the other hand, the proposed method is very simple and efficient: the calculations are very fast as the coefficients does not depend on time, whereas the accuracy is still acceptable.

In that case, considering $P = 20$ and $N = 200$ is not really efficient. However, it turns out that running 200 simulations takes only 3 seconds. If the numerical cost of one simulation had been much more, such a number of simulations would not have been affordable: it is the main drawback of non-intrusive methods. Fig. 11 shows that $P = 15$ and $N = 100$ still give quite good results.

About 65 % of the N POD modes were kept in the model, which is quite high. It is interesting to notice that with the "99 %" criterion, the number of POD modes is divided

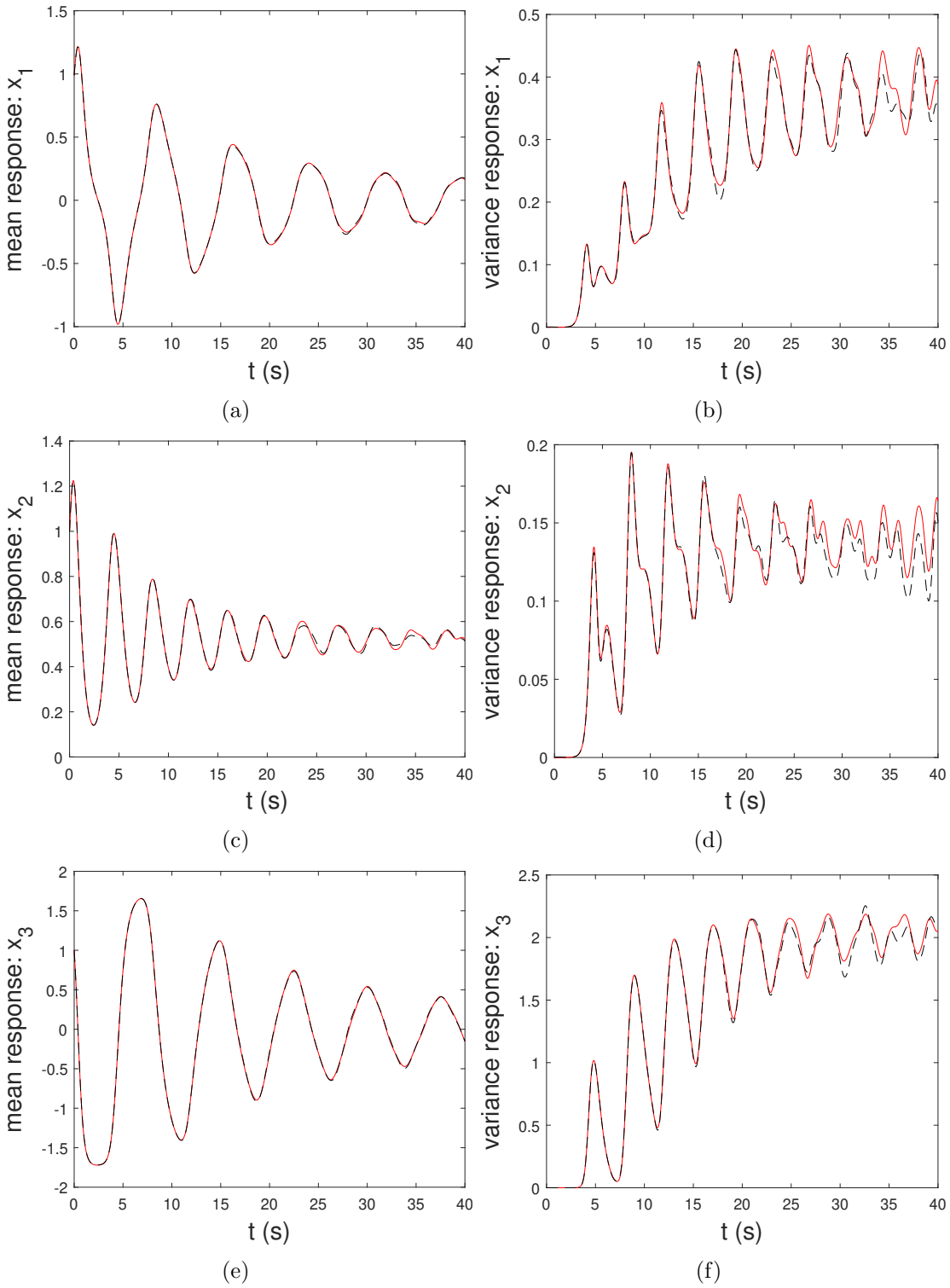

Figure 9: α=0.99; MCS (red solid line) vs. POD-PC method (black dashed line): x_1: mean (a), variance (b) - x_2: mean (c), variance (d) - x_3: mean (e), variance (f)

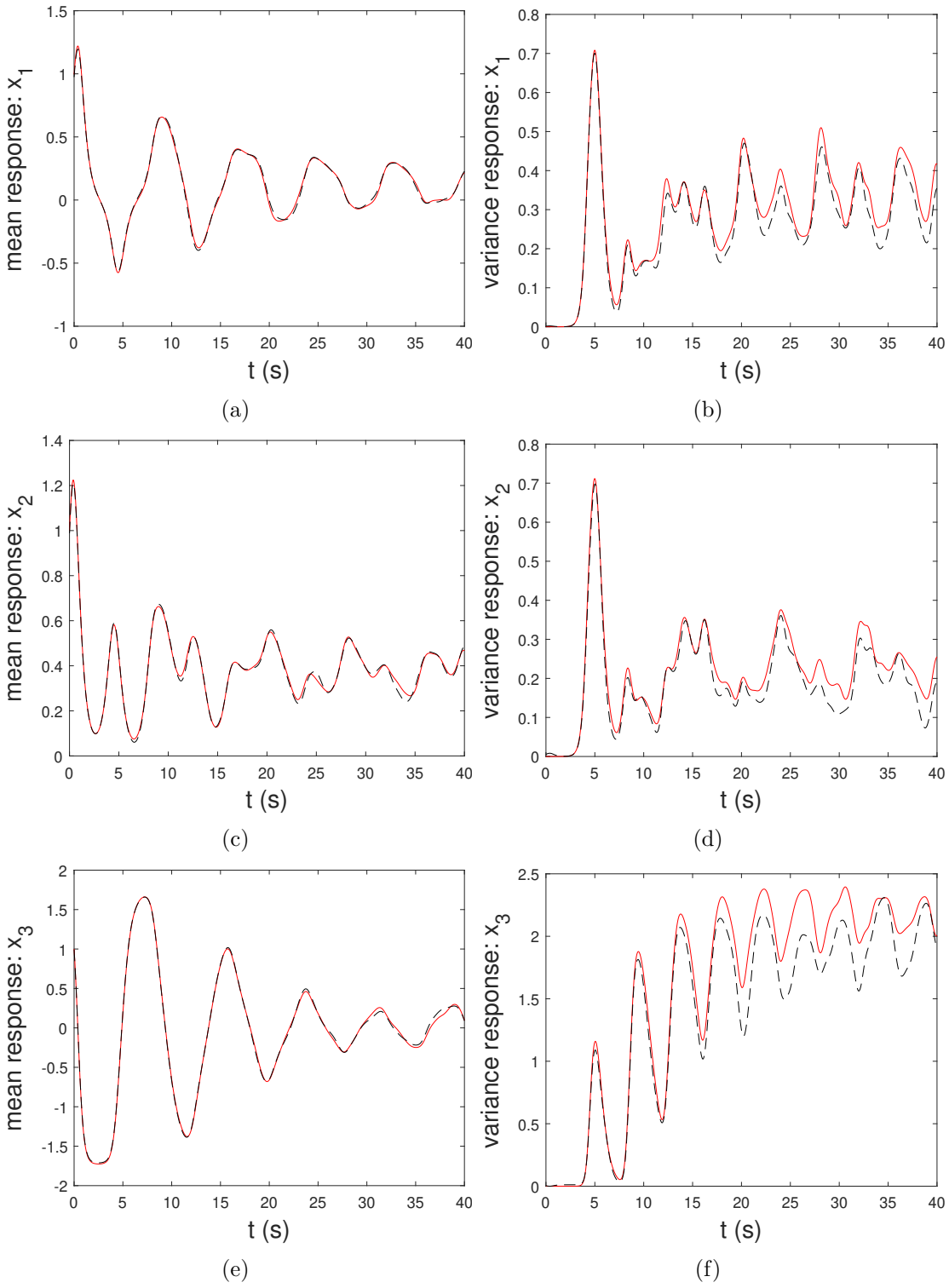

Figure 10: α=0.995; MCS (red solid line) vs. POD-PC method (black dashed line): x_1: mean (a), variance (b) - x_2: mean (c), variance (d) - x_3: mean (e), variance (f)

by two and the results obtained were very similar to the ones with the $\lambda_i/\lambda_{max} > 10^{-5}$ criterion. However, it is noticeable that beyond the 20-th POD-mode, the PCE of the coefficients given in Eq. (11) was very sparse: often, only 2 or 3 terms were required, whereas the PCE was not sparse for some of the very first mode coefficients. Therefore, the total number of PCE coefficients is only reduced by 30 %.

5. Conclusions

The non intrusive POD-PC model was presented to study random dynamical systems. Most of the current metamodel used to describe such systems require to compute the coefficient of the metamodel at each time step, which may be time demanding. Conversely, the POD-PC model separates the time and the random variables. Therefore, the number of PCE coefficients to be calculated does not depend on the number of time step but on the number of initial simulations required to identify the model. Furthermore, the POD extracts the main components of the signal and then reduces this number.

The examples show that this model works very well when the response shape does not vary much or vary smoothly with the variation of the random parameters. In fact, the amplitudes and the phases of the responses are affected by the randomness and then the coherent structures tend to disappear after some time. As the POD is based on the coherent structures of signals, it can then be expected that this can induce a lost of accuracy for a long-time integration.Therefore, the POD-PC model seems more adapted for simulating the transient response than the steady-state response of an uncertain dynamical system.

This model is simple and fast to implement as it only requires a singular value decomposition to account for the time and a polynomial interpolation to deal with the uncertainties. The examples showed that a quite high polynomial degree is often required to describe the randomness of the first POD-mode coefficients, which may be a drawback when many uncertain parameters are involved in describing the random dynamical system.

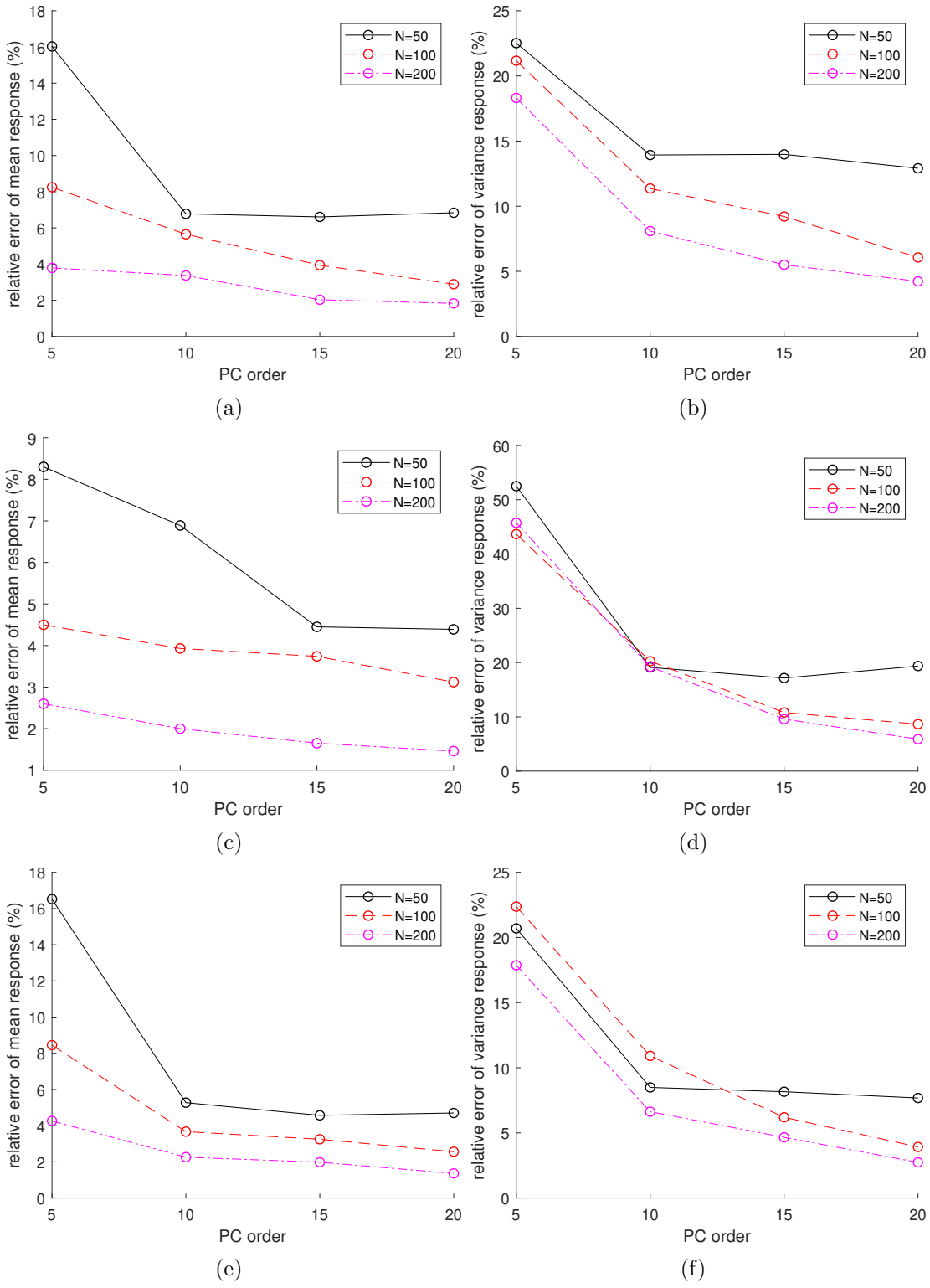

Figure 11: α=0.990; mean response relative error (x_1: (a), x_2: (c), x_3: (e)) and variance response relative error (x_1: (b), x_2: (d), x_3: (f)) in function of the PC order and for several initial numbers of samples: black solid line $N = 50$, red dashed line $N = 100$, magenta dash-dotted line $N = 200$

Acknowledgements

E. Jacquelin acknowledges the financial support from University of Lyon 1 for his 1-year academic sabbatical leave. This research was performed at the University of Florence.

References

[1] R. G. Ghanem, P. D. Spanos, Stochastic Finite Elements: A Spectral Approach, Springer-Verlag, New York, USA, 1991.

[2] A. Kundu, S. Adhikari, Transient response of structural dynamic system with parametric uncertainty, Journal of Engineering Mechanics 140 (2) (2014) 1–18.

[3] E. Jacquelin, O. Dessombz, J. J. Sinou, S. Adhikari, M. I. Friswell, Polynomial chaos-based extended Padé expansion in structural dynamics, International Journal for Numerical Methods in Engineering 111 (12) (2017) 1170–1191.

[4] C. Pettit, P. Beran, Spectral and multiresolution Wiener expansions of oscillatory stochastic processes, Journal of Sound and Vibration 294 (2006) 752–779.

[5] O. Le Maître, L. Mathelin, O. Knio, M. Hussaini, Asynchronous time integration for polynomial chaos expansion of uncertain periodic dynamics, Discrete & Continuous Dynamical System - Series A 28(1) (2010) 199–226.

[6] M. Gerritsma, J.-B. Van der Steen, P. Vos, G. Karniadakis, Time-dependent generalized polynomial chaos, Journal of Computational Physics 229 (2010) 8333–8363.

[7] J. Witteveen, H. Bijl, An unsteady adaptive stochastic finite elements formulation for rigid-body fluid–structure interaction, Computers and Structures 86 (2008) 2123–2140.

[8] J. Witteveen, H. Bijl, An alternative unsteady adaptive stochastic finite elements formulation based on interpolation at constant phase, Computers Methods and Applied Mechanics in Engineering 198 (2008) 578–591.

[9] C. Mai, B. Sudret, Surrogate models for oscillatory systems using sparse polynomial chaos expansions and stochastic time warping, Journal for Uncertainty Quantification 5 (1) (2017) 540–571.

[10] M. Bayarri, J. Berger, J. Cafeo, G. Garcia-Donato, F. Liu, J. Palomo, R. Parthasarathy, R. Paulo, J. Sacks, D. Walsh, Computer model validation with functional output, The Annals of Statistics 35 (5) (2007) 1874–1906.

[11] M. Spiridonakos, E. Chatzi, Metamodeling of dynamic nonlinear structural, Computers & Structures 157 (2015) 99–113.

[12] C. Mai, M. Spiridonakos, E. Chatzi, B. Sudret, Surrogate modeling for stochastic dynamical systems by combining nonlinear autoregressive with exogenous input models and polynomial chaos expansions, International Journal for Uncertainty Quantification 6(4) (2016) 313–339.

[13] F. Chinesta, P. Ladeveze, E. Cueto, A short review on model order reduction based on proper generalized decomposition, Archives of Computational Methods in Engineering 18 (2011) 395–404.

[14] A. Nouy, A generalized spectral decomposition technique to solve a class of linear stochastic partial differential equations, Computer Methods in Applied Mechanics and Engineering 196 (2007) 4521–4537.

[15] A. Nouy, A priori model reduction through proper generalized decompositionfor solving time-dependent partial differential equations, Computer Methods in Applied Mechanics and Engineering 199 (2010) 1603–1626.

[16] D. Higdon, J. Gattiker, B. Williams, M. Rightley, Computer model calibration using high-dimensional output, Journal of the American Statistical Association 103 (482) (2008) 570–583.

[17] G. Blatman, B. Sudret, Sparse polynomial chaos expansions of vector-valued response quantities, ICOSSAR, New York, USA, 2013.

[18] M. Guo, J. Hesthaven, Data-driven reduced order modeling for time-dependent problems, Computer Methods in Applied Mechanics and Engineering 345 (2019) 75–99.

[19] D. Xiu, Numerical Methods for Stochastic Computations – A Spectral Method Approach, Princeton University Press, 2010.

[20] B. Efron, T. Hastie, I. Johnstone, R. Tibshirani, Least angle regression, The Annals of Statistics 32 (2) (2004) 407–499.

[21] G. Blatman, B. Sudret, An adaptive algorithm to build up sparse polynomial chaos expansions for stochastic finite element analysis, Probabilistic Engineering Mechanics 25 (2) (2010) 183 – 197.

[22] G. Blatman, B. Sudret, Adaptive sparse polynomial chaos expansion based on least angle regression, Journal of Computational Physics 230 (6) (2011) 2345–2367.

[23] J. Drugowitsch, Variational bayesian inference for linear and logistic regression, arXiv:1310.5438v3 [stat.ML].

[24] C. Bishop, Pattern recognition and machine learning, Springer, 2006.

[25] W. R. Jacobs, T. Baldacchino, T. Dodd, A. S. R., Sparse bayesian nonlinear system identification using variational inference, IEEE Transactions on Automatic Control 63 (12) (2018) 4172–4187.

[26] D. Xiu, G. Karniadakis, The Wiener-Askey polynomial chaos for stochastic differential equations, SIAM Journal on Scientific Computing 24(2) (2002) 619–644.

[27] D. Xiu, G. Karniadakis, Modeling uncertainty in flow simulations via generalized polynomial chaos, Journal of Computational Physics 187 (2003) 137–167.

[28] E. Jacquelin, S. Adhikari, J.-J. Sinou, M. I. Friswell, The polynomial chaos expansion and the steady-state response of a class of random dynamic systems, ASCE Journal of Engineering Mechanics 141(4) (2015) 04014145.

[29] S. S. Isukapalli, R. Amit, P. Georgopoulos, Stochastic response surface methods (SRSMs) for uncertainty propagation: Application to environmental and biological systems, Risk Analysis 18 (3) (1998) 351–363.

[30] S. S. Isukapalli, Uncertainty analysis of transport-transformation models, Ph.D. thesis, The State University of New Jersey (1999).

[31] M. Berveiller, B. Sudret, M. Lemaire, Stochastic finite elements: a non intrusive approach by regression, European Journal of Computational Mechanics 15 (1-3) (2006) 81–92.

[32] L. Sirovich, Turbulence and the dynamics of coherent structures. part 1: Coherent structures, Quarterly of Applied Mathematics XLV(3) (1987) 561–571.

[33] B. Feeny, R. Kappagantu, On the physical interpretation of proper orthogonal modes in vibration, Journal of Sound and Vibration 211(4) (1998) 607–616.

[34] A. Chatterjee, An introduction to the proper orthogonal decomposition, Current Science 78 (7) (2000) 808–817.

[35] X. Ma, M. Azeez, A. Vakakis, Computer model calibration using high-dimensional output, Mechanical Systems Signal Processing 14 (2000) 37–48.

[36] M. Azeez, A. Vakakis, Proper orthogonal decomposition (pod) of a class of vibroimpact oscillations, Journal of Sound and vibration 240 (5) (2001) 859–889.

[37] ECE22.05, Uniform provisions concerning the approval of protective helmets and of their visors for drivers and passengers (2002).

[38] A. Pratellesi, S. Turrin, T. Haag, A. Scippa, N. Baldanzini, On the effect of testing uncertainties in the homologation tests of motorcycle helmets according to ece 22.05, International Journal of Crashworthiness 16 (5) (2011) 523–536.

[39] B. Chouvion, E. Sarrouy, Development of error criteria for adaptive multi-element polynomial chaos approaches, Mechanical Systems and Signal Processing 66-67 (2016) 201–222.

[40] V. Heuveline, M. Schick, A hybrid generalized polynomial chaos method for stochastic dynamicsal systems, International Journal for Uncertainty Quantification 4 (1) (2014) 37–61.

[41] S. Orszag, L. Bissonnette, Dynamical properties of truncated wiener–hermite expansions, The Physics of Fluids 10 (12) (1967) 2603–2613.